

Quasinormal-mode expansion of the scattering matrix

F. Alpeggiani,^{1,2} P. Nikhil,¹ E. Verhagen,¹ and L. Kuipers^{1,2}

¹*Center for Nanophotonics, FOM Institute AMOLF,
Science Park 104, 1098 XG Amsterdam, The Netherlands*

²*Kavli Institute of Nanoscience, Department of Quantum Nanoscience,
Delft University of Technology, Lorentzweg 1, 2628 CJ Delft, The Netherlands*

(Dated: February 28, 2023)

It is well known that the quasinormal modes (or resonant states) of photonic structures can be associated with the poles of the scattering matrix of the system in the complex-frequency plane. In this work, the inverse problem, i.e., the reconstruction of the scattering matrix from the knowledge of the quasinormal modes, is addressed. We develop a general and scalable quasinormal-mode expansion of the scattering matrix, requiring only the complex eigenfrequencies and the *far-field* properties of the eigenmodes. The theory is validated by applying it to illustrative nanophotonic systems with multiple overlapping electromagnetic modes. The examples demonstrate that our theory provides an accurate first-principle prediction of the scattering properties, without the need for postulating *ad-hoc* nonresonant channels.

Scattering matrices have been playing a ubiquitous role in physics since the early history of quantum field theory [1]. Nowadays, scattering-matrix techniques represent an irreplaceable tool for scientists working in nuclear physics [2], electronic transport [3], or classically chaotic systems [4], just to mention some of the several fields of application. Scattering matrices also enjoy a well deserved popularity in electromagnetic modeling, ranging from microwave devices [5] to nanophotonics applications, such as scattering and transmission from nanostructured objects [6–8].

Most of the systems that are usually investigated with scattering-matrix techniques display a highly structured resonant response as a function of the excitation frequency (or energy), with the resonances in the spectrum being directly related to the poles of the analytical continuation of the scattering matrix in the complex-frequency plane [9, 10]. For electromagnetic systems, such poles correspond to quasinormal modes (also called resonant states), i.e., complex-frequency solutions of Maxwell’s equations with outgoing-wave boundary conditions [11–15]. In a sense, quasinormal modes represent the bare skeleton around which the frequency-dependent response of the system is built. The interplay among different electromagnetic modes has proven to be crucial for explaining several intriguing phenomena, such as Fano resonances in optical systems [16], scattering dark states [17, 18], and the optical analog of electromagnetically induced transparency and superscattering [19], and for designing new optical materials, such as optical metasurfaces for wavefront shaping [20]. For these reasons, it is desirable and extremely interesting to be able to reconstruct *ab initio* the entire scattering matrix of a system from the knowledge of its quasinormal modes. Not only would such quasinormal-mode expansion contribute to the understanding of complicated spectral features in terms of interference and superposition of resonant states, but it would also offer practical advantages from the numerical point of view, since a full eigenmode calculation is generally faster and more comprehensive

than a large number of single-frequency simulations.

A promising theoretical platform in which to carry out this program is represented by temporal coupled-mode theory for optical resonators. Such framework has been fruitfully employed to study the transmission of layered photonic-crystal structures [16, 21, 22], gratings [23], coupled cavities and waveguides [24, 25], and the scattering cross section of nanoparticles [17, 26, 27]. For the moment, however, coupled-mode theory has been typically restricted to a selection of only one or two modes of the optical system. The residual spectral response is accounted for by a slowly varying frequency-dependent background, which is typically fitted from simulation data [16, 21, 22, 24]. Part of the difficulty in expanding coupled-mode theory by including an arbitrary number of modes lies in estimating the coupling coefficients that relate the resonant states with the input–output channels. For a small number of modes, these can be obtained from symmetry considerations [16, 24] or from the temporal decay rates [22]. However, in order to address the general case of multiple modes and an arbitrary configuration of input–output channels, a direct connection between the parameters of coupled-mode theory and the far-field properties of quasinormal modes is required.

In this work, we establish such a connection and we present a general theory to expand the scattering matrix on the quasinormal modes of photonic systems, which can be directly scaled to any number of eigenmodes and incoming or outgoing channels. The theory, based on the far-field asymptotic behavior of the modes and the unitarity property of the scattering matrix, represents a fully predictive tool that does not require the fitting of an additional nonresonant background. There are formal similarities between our results and the expansion of the electromagnetic Green function on quasinormal modes, which is a well known result from classical electrodynamics [11, 28, 29]; of course, when the expansion of the Green function is known for any point in space, then the scattering properties of the system can also be obtained [29, 30]. However, the usual quasinormal-mode theory

requires a global integration of the eigenfield over the entire space in order to calculate the modal normalization factors [12–14]. Conversely, the theory that we present significantly differs from these approaches in being completely independent of the choice of the normalization and requiring only the far-field asymptotic behavior of the modes, as opposed to the full spatial distribution of the eigenfield. All these characteristics make it particularly suitable for first-principle numerical simulations, especially for systems with a large number of overlapping quasinormal modes. Notably, since the formalism is derived on the basis of general coupled-mode theory, its range of applicability goes beyond that of classical electrodynamics.

The work is organized as follows. In Sec. I we derive the quasinormal-mode expansion of the scattering matrix, whereas in Sec. II we numerically validate the theory in the illustrative cases of photonic crystal slabs and multilayered metallic nanoparticles.

I. THEORY

A. Quasinormal modes

In order to provide a rigorous motivation for the application of the formalism of coupled-mode theory to optical systems, we begin our analysis by establishing a direct connection with the theory of quasinormal modes. We consider a system of dielectric or absorbing photonic structures, described by a spatially inhomogeneous distribution of the dielectric function $\varepsilon(\mathbf{r}, \omega)$. We assume that in the limit $\mathbf{r} \rightarrow \infty$, the dielectric function $\varepsilon(\mathbf{r}, \omega)$ tends to the constant value ε_b and we define $\Delta\varepsilon(\mathbf{r}, \omega) = \varepsilon(\mathbf{r}, \omega) - \varepsilon_b$ [31]. The system supports a discrete number of quasinormal modes (also called resonant states) which are defined as the complex-frequency solutions $\tilde{\mathbf{E}}_j$ of Maxwell's wave equation,

$$\nabla \times \nabla \times \tilde{\mathbf{E}}_j(\mathbf{r}) - \varepsilon(\mathbf{r}, \tilde{\omega}_j) \frac{\tilde{\omega}_j^2}{c^2} \tilde{\mathbf{E}}_j(\mathbf{r}) = 0, \quad (1)$$

with outgoing radiation boundary conditions [12–15]. As a consequence of the complex eigenfrequency $\tilde{\omega}_j$, quasinormal modes are characterized by a diverging amplitude in the far field. The modal eigenfields form a complete basis inside the structure, i.e., in the region where $\Delta\varepsilon(\mathbf{r}, \omega) \neq 0$, provided that $\Delta\varepsilon(\mathbf{r}, \omega)$ or any order of its derivative is discontinuous at the boundary of its domain [11, 28].

Following the usual scattering theory, we suppose that the system is illuminated by an incident field \mathbf{E}_b , which, in turn, is a solution of the wave equation (1) with only the background dielectric constant, ε_b . Splitting the total field in the incident and scattered components, $\mathbf{E}(\mathbf{r}) = \mathbf{E}_b(\mathbf{r}) + \mathbf{E}_s(\mathbf{r})$, the latter can be shown to satisfy the inhomogeneous wave equation in the presence of a source

term proportional to the incident radiation, i.e.,

$$\nabla \times \nabla \times \mathbf{E}_s(\mathbf{r}) - \varepsilon(\mathbf{r}, \omega) \frac{\omega^2}{c^2} \mathbf{E}_s(\mathbf{r}) = \Delta\varepsilon(\mathbf{r}, \omega) \frac{\omega^2}{c^2} \mathbf{E}_b(\mathbf{r}). \quad (2)$$

Limiting ourselves to the region where $\Delta\varepsilon \neq 0$, we can exploit the completeness property discussed above and expand the scattered field on the basis of quasinormal modes $\tilde{\mathbf{E}}_j$,

$$\mathbf{E}_s(\mathbf{r}) = \sum_j a_j \tilde{\mathbf{E}}_j(\mathbf{r}). \quad (3)$$

The exact expression for the coefficients a_j depends on the incident field. Eventually, the knowledge of \mathbf{E}_s in a finite region is sufficient to extract the far-field properties of the scattered field, as it is described by the same Eq. (2), which becomes

$$\nabla \times \nabla \times \mathbf{E}_s(\mathbf{r}) - \varepsilon_b \frac{\omega^2}{c^2} \mathbf{E}_s(\mathbf{r}) = \Delta\varepsilon(\mathbf{r}, \omega) \frac{\omega^2}{c^2} [\mathbf{E}_b(\mathbf{r}) + \mathbf{E}_s(\mathbf{r})].$$

This equation has the formal solution

$$\mathbf{E}_s(\mathbf{r}) = \int d^3\mathbf{r}' \left[\Delta\varepsilon(\mathbf{r}', \omega) \frac{\omega^2}{c^2} [\mathbf{E}_b(\mathbf{r}') + \sum_j a_j \tilde{\mathbf{E}}_j(\mathbf{r}')] \tilde{\mathbf{G}}_b(\mathbf{r}, \mathbf{r}', \omega) \right], \quad (4)$$

with $\tilde{\mathbf{G}}_b(\mathbf{r}, \mathbf{r}', \omega)$ being the dyadic Green tensor of the background electromagnetic environment with homogeneous dielectric constant ε_b . Since the integral in Eq. (4) is limited to the region where $\Delta\varepsilon \neq 0$, we were able to replace the field expansion of Eq. (3).

At this point, we expand the input field over a set of incoming waves (or, more generally, ports), $\mathbf{E}_b(\mathbf{r}) = \sum_{\alpha} s_{+\alpha} \mathbf{E}_{\alpha}^{(+)}$, and total electric field over a corresponding set of outgoing waves, $\mathbf{E} = \sum_{\alpha} s_{-\alpha} \mathbf{E}_{\alpha}^{(-)}$, whose detailed expression depends on the specific geometry of the system. Equation (4) clearly shows that the amplitude of each outgoing wave, $s_{-\alpha}$, can be written as the sum of a direct channel, which is directly proportional to the incoming amplitudes $s_{+\alpha}$, and a resonance-mediated channel, which is proportional to the quasinormal-mode amplitudes a_j . In turn, the latter amplitudes are related to the incoming field through Eq. (2). From the linearity of Maxwell equations, it follows that all these relations can be written in terms of linear operators. This is the basis of the coupled-mode formalism, which we illustrate in the following.

B. Coupled-mode equations

Seeking a more general formulation, we write the characteristic equation of quasinormal modes, Eq. (1), as an eigenvalue problem for the effective “Hamiltonian” $\Omega + i\Gamma$,

$$(\Omega + i\Gamma)\mathbf{a}_j = \tilde{\omega}_j \mathbf{a}_j, \quad (5)$$

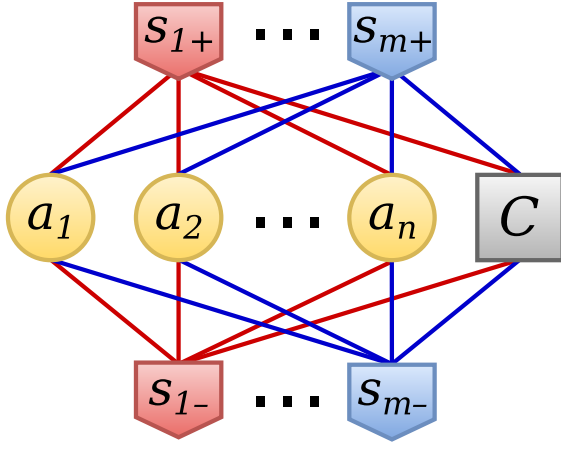


Figure 1. (Color online) Schematic of m ports coupled to n quasinormal modes with amplitudes a_j ($j = 1, \dots, n$) and linked by a direct-coupling term C . The notation s_{p+} and s_{p-} ($p = 1, \dots, m$) refers to the amplitude of incoming and outgoing waves, respectively.

where \mathbf{a}_j is the modal amplitude eigenvector associated to the complex eigenvalue $\tilde{\omega}_j$. Here and in the following, we assume the convention $\exp(i\omega t)$ for the temporal dependence of the field. Due to the inherently dissipative nature of quasinormal modes, the Hamiltonian operator $\Omega + i\Gamma$ is non-Hermitian and it has been split in the Hermitian and skew-Hermitian parts, which are expressed in terms of the two Hermitian operators Ω and Γ . Using the same language of Eq. (5) and following our previous considerations, we relate the incoming and outgoing amplitudes of the electromagnetic field (which we express in vector form as \mathbf{s}_+ and \mathbf{s}_-) by means of a system of coupled-mode equations:

$$i\omega \mathbf{a} = i(\Omega + i\Gamma)\mathbf{a} + K^T \mathbf{s}_+ \quad (6)$$

$$\mathbf{s}_- = C\mathbf{s}_+ + D\mathbf{a}. \quad (7)$$

The operator C represents the direct-coupling channel, whereas the operators K and D account for coupling between quasinormal modes and the incoming and outgoing ports, respectively. Although there might be in principle infinitely many quasinormal modes and ports, for practical reasons we assume that the number of modes and ports is truncated to the finite values n and m , respectively. In this way, all the operators reduce to finite-size matrices. The set of Eqs. (6) and (7) is summarized by the scheme in Fig. 1.

As originally demonstrated in Refs. [16] and [24], some relations among the quantities that appear in Eqs. (6) and (7) can be directly deduced from some very general physical properties of the system. First, electromagnetic reciprocity and energy conservation imply that

$$K = D \quad (8)$$

and

$$\Gamma = \frac{1}{2}D^\dagger D + \Gamma_{\text{nr}}, \quad (9)$$

respectively. In Eq. (9), we have straightforwardly extended the theory to include the (Hermitian) decay matrix Γ_{nr} , which accounts for absorption and other potential nonradiative-dissipation channels. Moreover, by comparing the dynamics described by Eqs. (6) and (7) with the time-reversed case and employing time-reversal symmetry, it can be shown that

$$CD^* = -D. \quad (10)$$

The system in Eqs. (6) and (7) has been extensively used to model the scattering properties of various photonic structures [17, 21, 22, 24, 27], proving itself particularly valuable for investigating the physical mechanism at the basis of various phenomena, such as the formation of Fano lineshapes in the spectrum as a consequence of the interference between the resonant and the direct-coupling channels [16]. In all these cases, however, the number of modes included in the equations is limited to one or two, and the direct-coupling channel, if present, is accounted for by fitting a specific frequency-dependent background response from independent numerical simulations of the spectrum (see, for instance, Refs. [16, 24, 27]). The need for independent external simulations prevents coupled-mode theory from providing a first-principle prediction of the scattering spectrum. However, in the light of our previous considerations in Sec. I A on the completeness of quasinormal modes, we expect that this limitation can be overcome by enlarging the set of electromagnetic modes under consideration, including also the resonances associated with the background, which are usually leaky modes with large decay rates. The formalism that we present in the next section is particularly suitable for implementing this strategy, as it is easily scalable to multiple modes with varying decay rates.

C. Expansion of the scattering matrix

The scattering matrix of the system connects the amplitude of the outgoing waves with the amplitude of the incoming waves:

$$S = C - iD(\omega\mathbb{I} - \Omega - i\Gamma)^{-1}D^T, \quad (11)$$

where we used identity (8). Here, we derive an expression for the expansion of the scattering matrix on quasinormal modes, on the basis of the system of Eqs. (6)–(7).

To this purpose, in addition to the complex eigenfrequencies of the quasinormal modes, $\tilde{\omega}_j$ ($j = 1, \dots, n$), we also assume the knowledge of the asymptotic behavior of the quasinormal-mode eigenfield in the output ports, which is equivalent to the knowledge of the relative complex amplitudes of the vectors

$$\mathbf{b}_j \doteq \mathbf{s}_-|_{\omega=\tilde{\omega}_j} = D\mathbf{a}_j. \quad (12)$$

For simplicity, we will refer to the vectors \mathbf{b}_j as the “scattering eigenvectors” of the system. As it is the case for all

eigenproblems, the (complex) normalization constant of the eigenvectors can be set arbitrarily; however, as proved in App. C, the final expression for the scattering matrix does not depend on the choice of such constant. As a consequence, our approach is inherently normalization-free, at variance with other works dealing with the expansion of the dyadic Green function, which require the quasinormal modes to be normalized in a specific fashion [13–15]. We stress that the scattering eigenvectors depend only on the far-field behavior of the resonant states and, thus, they can be obtained without computing the full distribution of the electromagnetic field over all space. This characteristic is particularly helpful, for instance, when quasinormal modes are calculated with numerical techniques such as the boundary-element method or the multipole expansion method, which typically benefit from a faster rate of convergence for far-field calculations.

Since the matrix $\Omega + i\Gamma$ is not Hermitian, the right eigenvectors alone are not orthogonal. However, as it is known from the theory of complex Hamiltonians [32], right eigenvectors (\mathbf{a}_j in our case) form a biorthogonal basis together with left eigenvectors, which are defined by the equation

$$\mathbf{l}_j^\dagger(\Omega + i\Gamma) = \tilde{\omega}_j \mathbf{l}_j^\dagger. \quad (13)$$

To simplify the notation, we introduce the $n \times n$ matrix A whose columns are the right eigenvectors \mathbf{a}_j and the corresponding matrix L of the column left eigenvectors \mathbf{l}_j . With this new notation, Eq. (5) becomes:

$$(\Omega + i\Gamma)A = A\tilde{\Omega}, \quad (14)$$

with $\tilde{\Omega}$ being the diagonal matrix of the complex eigenvalues $\tilde{\omega}_j$. Moreover, we define the $m \times n$ matrix B whose columns are the vectors \mathbf{b}_j .

The complex Hamiltonian of Eq. (5) can then be expanded on the biorthogonal basis as follows [32]:

$$\omega\mathbb{I} - \Omega - i\Gamma = A(\omega\mathbb{I} - \tilde{\Omega})L^\dagger. \quad (15)$$

Even if the right eigenvectors are not orthogonal, they are however linearly independent [32]; thus, we can formally write $L = (A^\dagger)^{-1}$. Replacing Eq. (15) into Eq. (11), we obtain the quasinormal-mode expansion of the scattering matrix,

$$S = C - iB \frac{1}{\omega\mathbb{I} - \tilde{\Omega}} \Lambda^{-1} B^T, \quad (16)$$

where we define $\Lambda \doteq A^T A$ and we use the relation $B = DA$, which comes directly from Eq. (12). For the moment, Eq. (16) represents only a formal result, which can be also seen as a special case of Mittag-Leffler's theorem on the pole-expansion of meromorphic functions [33]. For all practical purposes, it is crucial to derive an expression for the matrix Λ . This latter matrix plays a fundamental physical role, because the amplitude and phase of its terms determine the oscillator strength of each

resonance and affect the degree of interference among the modes, which, in turn, has been found responsible for the appearance of interesting spectral features, such as Fano lineshapes [16] or the optical analogue of electromagnetically-induced transparency [19].

First of all, it can be shown that Λ is diagonal. This result follows from the symmetry of the complex Hamiltonian $\Omega + i\Gamma$, which can be proved by combining Eqs. (9) and (10). The same result can also be derived from the requirement that the resulting scattering matrix must be symmetric [24]. Next, by multiplying each side of Eq. (10) by A^* and after some algebraic manipulations, we obtain $CB^* = -B\Lambda^{-1}(A^\dagger A)^*$, which we can recast in the more compact form

$$CB^* + B\Lambda^{-1}Q^* = 0, \quad (17)$$

which defines the matrix $Q = A^\dagger A$.

For simplicity, we assume that there is no absorption, i.e., $\Gamma_{nr} = 0$. The general absorbing case can be treated with some minor modifications and will be summarized in App. A. By multiplying Eq. (14) by A^\dagger on the left, taking the difference with its Hermitian conjugate, and employing Eq. (9), we arrive at

$$Q\tilde{\Omega} - \tilde{\Omega}^*Q = 2iA^\dagger\Gamma A = iA^\dagger D^\dagger D A = iB^\dagger B. \quad (18)$$

In general, the solution for Q cannot be written explicitly in terms of matrix products; however, it is straightforward to express it componentwise, as follows:

$$Q_{ij} = i \frac{\mathbf{b}_i^\dagger \mathbf{b}_j}{\tilde{\omega}_j - \tilde{\omega}_i^*}. \quad (19)$$

This latter equation allows us to clarify the physical meaning of Eq. (17). With the aid of Eqs. (16) and (19), it can be shown that Eq. (17) is equivalent to the condition

$$S^\dagger(\tilde{\omega}_j)\mathbf{b}_j = \mathbf{0}. \quad (20)$$

From the inversion of the scattering matrix, on the other hand, we obtain that $S^{-1}(\tilde{\omega}_j)\mathbf{b}_j = \mathbf{0}$, since quasinormal modes are defined as the self-sustaining solution of Maxwell's equations in the absence of any input radiation. Comparing the two results, it is clear that Eq. (17) guarantees that the scattering matrix is unitary at the modal eigenfrequencies, as required by energy conservation.

Equations (19) and (17) allow us to fully determine the matrix Λ , and, hence, the quasinormal-mode expansion of Eq. (16). However, a closer inspection of Eq. (17) reveals that the system has $m \times n$ equations (the dimension of B) and only n unknowns (the diagonal of Λ). Thus, for a given direct coupling matrix C , the system is generally overdetermined and a solution is not always guaranteed to exist. From a different perspective, the direct matrix C cannot be chosen freely, but it must satisfy some constraints that depend on the properties of the resonant

states. In practice, it might be difficult to choose a direct matrix with a simple analytical form and, at the same time, consistent with Eq. (17), especially when a large number of quasinormal modes is involved.

For all these reasons, it is essential to develop a general theory that encompasses also the case when the matrix C is an approximation of the exact direct-coupling matrix. To this end, instead of looking for an exact solution of Eq. (17), we search for an approximate solution in the least-square sense. To be more precise, having defined the vectors \mathbf{x}_j ($j = 1, \dots, n$) as the columns of the matrix

$$X = CB^*(Q^*)^{-1}, \quad (21)$$

we look for the diagonal matrix Λ in Eq. (17) whose diagonal terms, λ_j , minimize the objective function

$$f(\lambda_1, \dots, \lambda_n) = \sum_{j=1}^n |\lambda_j \mathbf{x}_j + \mathbf{b}_j|^2. \quad (22)$$

This reformulation of the problem does not affect the generality of the theory, because, if Eq. (17) has an exact solution, then such solution must coincide with the least-square one [34].

A simple calculation of the stationary points of the objective function leads to the result $\lambda_j = -\mathbf{x}_j^\dagger \mathbf{b}_j / (\mathbf{x}_j^\dagger \mathbf{x}_j)$, which, once replaced into Eq. (16), provides us with the final expression

$$S = C + i \sum_{j=1}^n \frac{\mathbf{x}_j^\dagger \mathbf{x}_j}{\mathbf{x}_j^\dagger \mathbf{b}_j} \frac{\mathbf{b}_j \mathbf{b}_j^T}{\omega - \tilde{\omega}_j}. \quad (23)$$

Equation (23), together with Eqs. (21) and (19), is the desired expansion of the scattering matrix and it represents the main result of the present work. Using Eq. (21), the expansion coefficients can be explicitly written as

$$\frac{1}{\lambda_j} = -\frac{\mathbf{x}_j^\dagger \mathbf{x}_j}{\mathbf{x}_j^\dagger \mathbf{b}_j} = -\frac{\sum_{nn'} Q_{nj}^{-1} (Q_{n'j}^{-1})^* \mathbf{b}_n^T C^\dagger C \mathbf{b}_{n'}}{\sum_n Q_{nj}^{-1} \mathbf{b}_n^T C^\dagger C \mathbf{b}_j}. \quad (24)$$

The denominator of the coefficient can be regarded as a modified inner product that renormalizes the scattering eigenvectors in order to guarantee the total scattering matrix to be unitary. In the limiting case when the off-diagonal elements of Q are negligible, the expression in Eq. (23) reduces to a modified version of the prominent Breit-Wigner formula of nuclear physics [2, 4], as shown in App. B. In addition, in App. C we also show that the result in Eq. (23) is independent of the normalization of the scattering eigenmodes.

II. APPLICATIONS

A. Photonic crystal slab

As an illustrative example, we consider a photonic crystal slab composed of a square lattice of circular holes

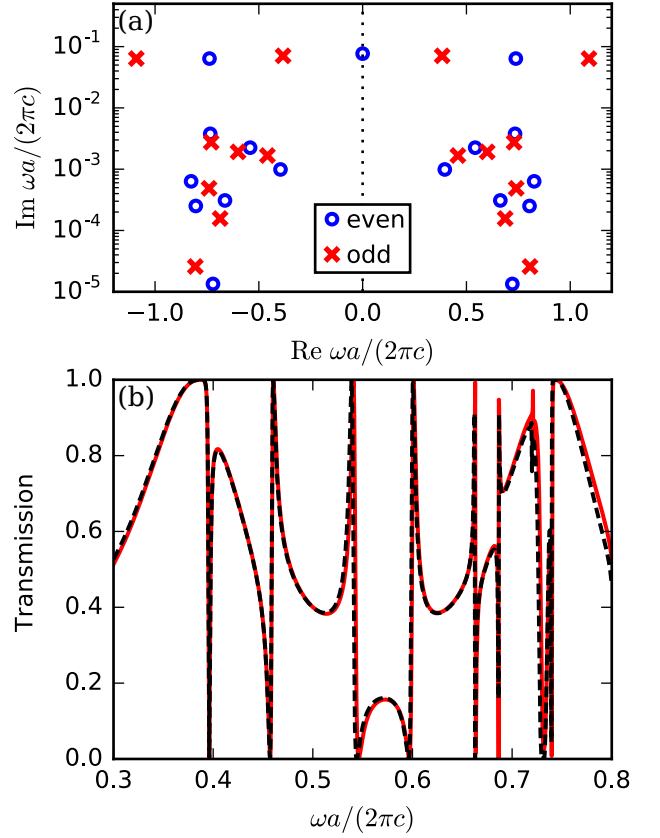


Figure 2. (Color online) Application of the theory to a photonic crystal slab composed of a square lattice of air holes etched in a suspended silicon membrane. (a) Real and imaginary part (log scale) of the quasinormal-mode complex eigenfrequencies, together with the corresponding symmetry of the modes (even, odd) by inversion with respect to the slab middle plane. (b) Transmission intensity computed by expanding the scattering matrix on the quasinormal modes (red solid line), compared with the exact result by the Fourier modal method (dashed line) [35].

etched in a silicon membrane ($\varepsilon = 12.1$). Indicating with a the lattice constant, we assume the slab thickness and the hole radius $t = 0.4a$ and $r = 0.2a$, respectively. For normally incident light polarized along one of the lattice axes, we can limit ourselves to a single polarization of light; moreover, in the range of frequency $\omega < 2\pi/a$, only the zeroth order of diffraction is available. As a consequence, the system can be effectively described with two ports, corresponding to the plane waves $E_{1,+} = s_{1,+} e^{-i\omega z/c}$ and $E_{2,+} = s_{2,+} e^{i\omega z/c}$, propagating along the normal direction to the slab, which we indicate as the z axis.

In Fig. 2(a) we show the complex eigenfrequencies of the quasinormal modes of the system for normally incident light. Although all the modes represent equally valid solutions of the same characteristic equation (1) and they are treated on equal grounds in the expansion of the scattering matrix (23), it is useful from a physical point of view to distinguish between two categories of quasi-

normal modes: weakly dissipating quasi-guided modes and leaky modes with much larger radiation rates. As it appears from Fig. 2(a), the threshold between the two families can be set around $\text{Im } \tilde{\omega} \approx 10^{-2} (2\pi c/a)$, with a difference of more than one order of magnitude between the corresponding imaginary parts of the eigenfrequencies. The leaky modes ($\text{Im } \tilde{\omega} > 10^{-2} 2\pi c/a$) have strong similarities with the Fabry-Pérot resonances of a homogeneous dielectric slab with an average refractive index n_{av} , displaying a roughly constant frequency spacing of the order of the free spectral range $\delta\omega = \pi c/(n_{\text{av}}t)$. The deviation from the equal spacing behavior grows when the frequency increases, due to the wavelength becoming more sensitive to the dielectric-function inhomogeneity in the system [21].

Quasi-guided modes can be easily computed in various ways, including, e.g., frequency-domain [14] or time-domain [13, 28] methods, or by determining the poles of the scattering or transmission coefficient in the complex frequency plane [9]. These techniques can also be combined, in order to exploit specific advantages. For instance, in the present example, the modes with $\text{Re } \tilde{\omega}_j > 0$ have been computed by solving a linearized version of the eigenproblem in Eq. (1) with a commercial finite-element package [36], whereas, for better numerical accuracy, leaky modes have been obtained separately by looking for the complex-frequency poles of the transmission amplitude computed with the Fourier modal method using a freely available solver [35]. Since the wave equation (1) is second order in the frequency, for each quasinormal mode with $\text{Re } \tilde{\omega}_j > 0$ there exists a corresponding state with $\tilde{\omega}_{j'} = -\tilde{\omega}_j^*$ and $\tilde{\mathbf{E}}_{j'}(\mathbf{r}) = \tilde{\mathbf{E}}_j^*(\mathbf{r})$ [11], which has been included in the calculations, raising the total number of quasinormal modes under consideration in this example to $n = 33$. Due to numerical difficulties in performing the calculations near the imaginary axis of the complex-frequency plane, the decay rate of the $\text{Re } \tilde{\omega}_j = 0$ mode has been estimated using the analytical formula for a homogeneous dielectric slab with an averaged refractive index [12].

The asymptotic behavior of the eigenfield is entirely determined by the inversion symmetry of the system with respect to the middle plane of the slab. Since the electric field amplitude is either even or odd with respect to the inversion, as indicated in Fig. 2(a), we can directly assume the scattering eigenvectors

$$\mathbf{b}_{\pm} = \frac{1}{\sqrt{2}} \begin{bmatrix} 1 \\ \pm 1 \end{bmatrix}. \quad (25)$$

for even (“+”) and odd (“−”) modes. As we already remarked, since the scattering matrix expansion is independent of the eigenfield normalization, any other choice of the normalization in Eq. (25) would have been equally suitable. Finally, in agreement with our considerations on the completeness of quasinormal modes for photonic systems, we take the 2×2 identity matrix as the direct-

coupling matrix

$$C = \mathbb{I}_{2 \times 2}. \quad (26)$$

In this way, we can derive the expression of the scattering matrix of the photonic crystal slab by applying Eq. (23) with the complex eigenfrequencies of Fig. 2(a) and the scattering eigenvectors of Eq. (25). The transmission intensity obtained from the resulting scattering matrix is shown by the solid curve in Fig. 2(b), and it is compared with an independent calculation by the Fourier modal method (dashed line) [35]. The agreement between the curves is excellent, highlighting the validity of the quasinormal-mode expansion of the scattering matrix. The comparison confirms that the first-principle description of the optical properties of the system provided by the theory is complete and accurate; moreover, we stress that such a description does not require any *ad-hoc* assumptions on the direct coupling channel and is based only on the complex eigenfrequencies of the quasinormal modes.

B. Asymmetric photonic crystal structure

A specific advantage of the scattering-matrix expansion is the straightforward applicability to generic systems lacking any particular symmetry. In order to illustrate this point, we consider a square lattice of L-shaped void structures partially patterned in a silicon slab. The shape and size of the structures is schematized in the inset of Fig. 3(a). The height of the patterned region ($h = 0.2a$) is one half of the total thickness of the slab ($t = 0.4a$), resulting in a configuration which is not symmetric by inversion along z . Moreover, for incident light polarized along one of the lattice main axes, the transmitted and reflected radiation will include a cross-polarized fraction. Therefore, we can model the system by defining four ports, corresponding to plane waves propagating above and below the slab and polarized along the two in-plane crystal axis (which we indicate as x and y). According to the completeness of the quasinormal modes, we assume the identity matrix as the direct-coupling matrix, i.e., $C = \mathbb{I}_{4 \times 4}$.

The complex eigenfrequencies of the quasinormal modes, computed with the finite-element method [36], are presented in Fig. 3(a). Even in this case we can distinguish between a set of quasi-guided modes and a set of roughly equispaced leaky modes with a larger dissipation rate. Similarly to the previous example, the decay rate of the pair of modes with $\text{Re } \tilde{\omega}_j = 0$ has been estimated using the analytical results for a homogeneous dielectric slab, and, moreover, we have also explicitly included the modes with $\tilde{\omega}_{j'} = -\tilde{\omega}_j^*$. However, in this case the scattering eigenvectors \mathbf{b}_j must be obtained from the asymptotic behavior of the calculated quasinormal-mode eigenfield [37]. To this purpose, we consider the x and y electric-field components of each quasinormal mode in two planes located above and below the silicon slab at a

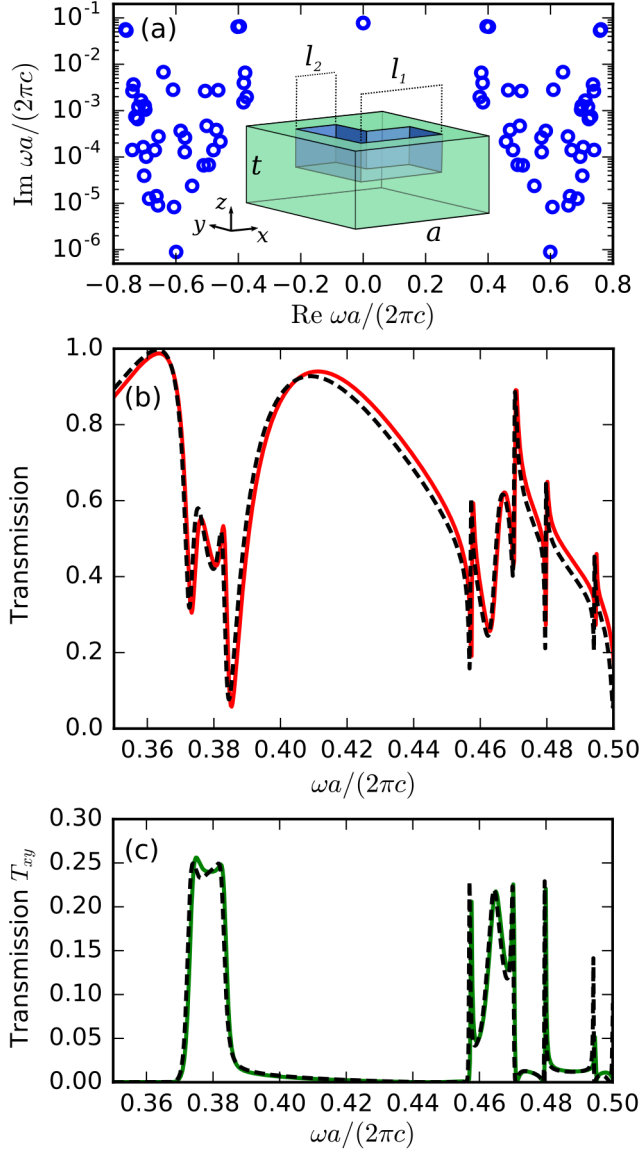


Figure 3. (Color online) (a) Circles: real and imaginary part (log scale) of the quasinormal-mode eigenfrequencies of a square lattice of L-shaped patterned structures in a silicon membrane. The unit cell of the structure is represented in the inset ($t = 0.4a$, $l_1 = 0.6a$, and $l_2 = 0.3a$). Note that the structure is not symmetric by inversion along the z axis. (b) Total transmittance, T , and (c) cross-polarized transmittance, T_{xy} , computed by expanding the scattering matrix on the quasinormal modes (solid line), compared with the exact result by the Fourier modal method (dashed line) [35].

sufficiently large distance to make the near-field contributions negligible. The specific choice of the distance does not affect the results, since only the relative amplitudes among the field components are relevant for the theory. It is interesting to note that the scattering eigenvector can also be computed with a near-to-far-field transformation of the quasinormal modes [38].

From the expansion of the scattering matrix in

Eq. (23), we computed the total transmission intensity, T , and the cross-polarized transmission intensity, T_{xy} (i.e., intensity of x -polarized transmitted light for y -polarized incident radiation). These quantities are shown (solid curves) in Figs. 3(b)–(c) and they are compared with the exact results (dashed curves) obtained from the Fourier modal method [35]. There is good agreement between the curves, especially in the vicinity of multiple narrow resonances, further confirming the validity of our approach as a predictive tool for computing the scattering matrix of electromagnetic systems. The small deviation from the exact result in the high-frequency region of Fig. 3(b) is likely due to the lower number of leaky modes included in this example with respect to the case of Sec. II A. The large radiative width of leaky modes (with a quality factor of the order of 10) implies that additional states beyond the frequency range under consideration may still have a small effect on the transmission in Fig. 3(b). To corroborate this hypothesis, we verified that the agreement with simulation data can be further improved when an additional pair of leaky modes at $\text{Re } \tilde{\omega}_j \simeq 1.1(2\pi c/a)$ is included in the scattering matrix expansion [37].

C. Layered metallic particle

In order to highlight the generality of the theory, we consider a very different example. As demonstrated in Refs. [17, 26, 27], coupled-mode theory can be used to model the scattering and absorption cross-sections of spatially confined scatterers, such as metallic nanoparticles. Although in these works only one or two quasinormal modes are included in the application of the theory, our formalism allows the extension of the number of modes and channels in a straightforward way. Moreover, we also use this example to illustrate the extension of the theory to include absorbing materials, which is summarized in App. A.

For three-dimensional scattering objects, the ports correspond to incoming and outgoing spherical waves of degree l , order m , and both transverse electric (TE) and transverse magnetic (TM) polarization [6]. For simplicity, we consider a spherically symmetric system, where we can limit ourselves only to multipole terms with $m = 1$ and $l > 0$ [6, 17]. The scattering and absorption cross section can be expressed as a function of the reflection coefficients, i.e., the diagonal terms of the scattering matrix, as follows [39]:

$$\sigma_{\text{sca}} = \sum_{\sigma} \sum_{l=1}^{\infty} \frac{\lambda^2}{8\pi} (2l+1) |1 - S_{l\sigma, l\sigma}|^2; \quad (27)$$

$$\sigma_{\text{abs}} = \sum_{\sigma} \sum_{l=1}^{\infty} \frac{\lambda^2}{8\pi} (2l+1) \left(1 - |S_{l\sigma, l\sigma}|^2\right) \quad (28)$$

(the index σ indicates polarization: $\sigma = \text{TE}, \text{TM}$). These expressions can be generalized to nonspherical scatterers

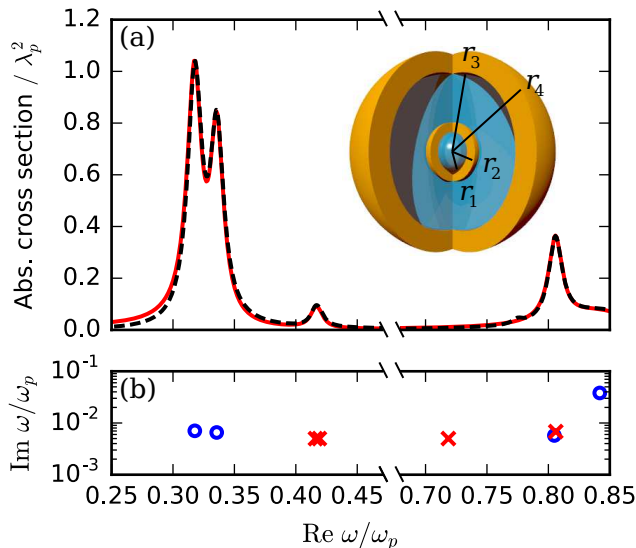


Figure 4. (Color online) (a) Absorption cross section of a multilayered spherical nanoparticle constituted of a dielectric core and alternating layers of a Drude metal and a dielectric ($\epsilon = 2.1$), as shown in the inset. The red solid line is obtained from the quasinormal-mode expansion, whereas the dashed curve is the exact result from generalized Mie theory. The values of the radii of the different layers, starting with the inner one, are $r_1 = 0.012\lambda_p$, $r_2 = 0.0186\lambda_p$, $r_3 = 0.138\lambda_p$, $r_4 = 0.18\lambda_p$, with all lengths being expressed in units of the plasma wavelength $\lambda_p = 2\pi c/\omega_p$. (b) Real and imaginary part of the quasinormal-mode eigenfrequencies included in the expansion. All modes are TM polarized. Circles and crosses refer to $l = 1$ and $l = 2$ modes, respectively, where l is the azimuthal number.

by including the additional dependence on the order m of the modes [27].

For the sake of illustration, we consider a multilayered spherical particle with alternating layers of dielectric ($\epsilon = 2.1$) and metallic materials, according to the structure sketched in the inset of Fig. 4. Core-shell metallic nanoparticles are a viable and well established platform for obtaining a significant local field enhancement together with a broad frequency tunability in the spectral response [40]. Here, we are mainly interested in the presence of multiple modes in each scattering channel, which underlines the advantages of our theoretical treatment in dealing with complex electromagnetic systems. Since we are considering a subwavelength particle sustaining plasmonic resonances, we limit ourselves to the lowest order TM-polarized modes ($l = 1$ and $l = 2$). We assume the metal dielectric function to follow Drude's model

$$\epsilon(\omega) = 1 - \frac{\omega_p^2}{\omega(\omega + i\kappa_{\text{nr}})} \quad (29)$$

with plasma frequency ω_p and nonradiative damping rate κ_{nr} . In all calculations, we assume $\kappa_{\text{nr}} = 0.01\omega_p$. This value is in agreement with those obtained from the fitting of the dielectric function of noble metals (e.g., gold) at frequencies lower than the onset of interband transitions

[14]. The complex eigenfrequencies of the modes have been extracted from the position of the poles of the exact reflection coefficient in the complex-frequency plane [39] and they are presented in Fig. 4(b).

In the presence of absorbing materials, the theory summarized in App. A requires the knowledge of the nonradiative decay rate of the modes, which is not directly available from our calculations, since the imaginary part of the complex eigenfrequency includes both the radiative and nonradiative components. In the case of low absorption, it is possible to distinguish the two contributions in an approximate way, by computing the complex eigenfrequencies twice, the second time upon setting Drude's damping rate to zero, and by taking the difference between the imaginary parts of the frequency in both calculations:

$$\gamma_{\text{nr},j} = \text{Im} \tilde{\omega}_j - \text{Im} \tilde{\omega}_j^{(\kappa_{\text{nr}}=0)}. \quad (30)$$

The absorption cross section of the multilayered particles as calculated with our theory [Eqs. (23) and (A2)] is depicted in Fig. 4(a) and it is compared with the exact result of generalized Mie theory [6, 39]. The agreement of the curves is excellent, especially considering the additional level of approximation involved in estimating the nonradiative decay rates. Notable spectral features, such as the dip around $\omega = 0.33\omega_p$, which is due to the interference between partially overlapping $l = 1$ modes, or the significantly different oscillator strengths of $l = 1$ and $l = 2$ modes, are well reproduced by the scattering matrix expansion. These results demonstrate that the theory can be easily extended to non-unitary systems, when an estimate of the radiative efficiency of each quasinormal mode is available.

III. DISCUSSION AND CONCLUSIONS

In this work, we derived a general approach to expand the scattering matrix of optical systems on the basis of quasinormal modes. We validated the theory with some illustrative examples, showing that the resulting scattering matrix is complete and does not require the fitting of an additional background. The only requirements of the theory are the knowledge of the complex eigenfrequencies and the far-field behavior of the electromagnetic modes, without the need to compute the full spatial distribution of the electromagnetic field. Furthermore, the results are independent of the choice of the eigenmode normalization.

Creating artificial optical materials is an important goal in current nanophotonic research [41]. Such materials allow us to precisely control the intensity, phase, and polarization of scattered and transmitted light and to enhance light-matter interaction at the nanoscale. Spatial arrangements of optical resonators have been used, for instance, to realize high-contrast gratings [42], photonic metasurfaces [20, 43, 44], and zero-refractive-index metamaterials [45]. When the constituting optical resonators

are chiral, several intriguing effects can be observed, such as the asymmetric transmission of circularly and linearly polarized light [46, 47]. Even for a single optical resonator, like a multilayered particle, the interference of different resonant states give rise to interesting phenomena, such as, for instance, the optical analog of electromagnetically induced transparency and superscattering [19] and the formation of scattering dark states [17, 18]. Multiple-resonance effects can also be exploited to tailor the scattering cross section of a scatterer, making it transparent to an outside observer [48]. All these optical systems are typically characterized by a complex spectral structure, due to the presence of multiple electromagnetic modes coupled to the environment via various incoming and outgoing channels.

Our theory establishes a direct connection between the electromagnetic modes and the spectral properties of photonic resonant systems. The expression for the quasinormal-mode expansion that we derive is reminiscent of the Breit-Wigner formula [2, 4], albeit with the some notable distinctions. A crucial difference is that the coefficient of each resonant term in the expansion depends on the frequencies and the amplitudes of all the other modes via a specifically introduced coupling matrix Q . This additional dependence reflects the fact that, whereas the application of the Breit-Wigner formula is restricted to non-overlapping resonances, no such limitation applies to the present theory, which accounts in a natural way for the effective interaction among different states originating from the coupling to a common external environment. For this reason, the theory is particularly suitable for investigating the physical mechanisms at the heart of highly structured spectra, such as those arising from the interference of several closely spaced modes. Indeed, as we noted above, this is the case for many photonic systems which are currently the subject of intense research efforts. At the same time, our formalism represents also a powerful and predictive tool for first-principle calculation of the scattering behavior of general physical systems.

ACKNOWLEDGMENTS

This work is part of the research program of the Foundation for Fundamental Research on Matter (FOM), which is part of the Netherlands Organisation for Scientific Research (NWO). The authors acknowledge support from the European Research Council (ERC Advanced Grant 240438-CONSTANS) and from an industrial partnership program between Philips and FOM.

Appendix A: Presence of absorption

In the presence of absorbing materials, the nonradiative term Γ_{nr} can be treated as a perturbation of the total Hamiltonian. Of course, this approach is rigorously

valid only in the low-dissipation limit. We can then apply first-order perturbation theory and write

$$(\Omega + i\Gamma - i\Gamma_{\text{nr}})A = A(\tilde{\Omega} - i\tilde{\Gamma}_{\text{nr}}), \quad (\text{A1})$$

where $\tilde{\Gamma}_{\text{nr}}$ is the diagonal matrix of the first-order nonradiative decay rates, $\gamma_{\text{nr},j}$ ($j = 1, \dots, n$). The derivation in Sec. IC can be adapted in a straightforward way, leading to the following generalized expression for the coupling matrix Q originally defined in Eq. (19):

$$Q_{ij} = i \frac{\mathbf{b}_i^\dagger \mathbf{b}_j}{\tilde{\omega}_j - i\gamma_{\text{nr},j} - \tilde{\omega}_i^* - i\gamma_{\text{nr},i}}. \quad (\text{A2})$$

The remaining part of the derivation remains unchanged, and final result for the scattering-matrix expansion is provided by the same Eq. (23).

Appendix B: Case of orthogonal modes

If the scattering amplitudes of the quasinormal modes are orthogonal (i.e., $\mathbf{b}_i^\dagger \mathbf{b}_j = 0$ for $i \neq j$), or the spectral overlap between the modes can be neglected, the coupling matrix Q of Eq. (19) becomes diagonal. The least-square solutions of Eq. (17) can, then, be written as $\lambda_j = -\mathbf{b}_j^T C^\dagger \mathbf{b}_j / (2\text{Im } \tilde{\omega}_j)$. As a result, the scattering-matrix expansion of Eq. (23) assumes the simpler expression:

$$S = C + 2i \sum_{j=1}^n \frac{\text{Im } \tilde{\omega}_j}{\omega - \tilde{\omega}_j} \frac{\mathbf{b}_j \mathbf{b}_j^T}{\mathbf{b}_j^T C^\dagger \mathbf{b}_j}. \quad (\text{B1})$$

This equation can be understood as a modified version of the Breit-Wigner formula [2, 4], in which the interaction between overlapping modes is neglected, but where the relation between the phase of each resonant term and the direct-coupling matrix C is retained.

Appendix C: Free choice of the normalization of the scattering amplitudes

In this last paragraph, we show that the result in Eq. (23) is independent of the normalization of the scattering amplitudes of the quasinormal modes. To this end, we consider a different set of amplitudes \mathbf{b}'_j , which differ from the original \mathbf{b}_j by some complex multiplicative constants ϕ_j (which can be different for different modes):

$$\mathbf{b}'_j = \phi_j \mathbf{b}_j. \quad (\text{C1})$$

Introducing the diagonal matrix $\Phi = \text{diag}(\phi_j)$ and the matrix Q' , defined by the expression in Eq. (19) with the modified eigenvectors, it is straightforward to verify that $Q = \Phi^{*-1} Q' \Phi^{-1}$. In a similar fashion, we observe that Eq. (17) retains exactly the same form provided that Q , B , and Λ are replaced by Q' , the column matrix of the new eigenvectors, B' , and $\Lambda' = \Phi \Lambda \Phi$, respectively. Then,

substituting these replacements in Eq. (16), we obtain that

$$S = C - iB \frac{1}{\omega\mathbb{I} - \tilde{\Omega}} \Lambda^{-1} B^T = C - iB' \frac{1}{\omega\mathbb{I} - \tilde{\Omega}} \Lambda'^{-1} B'^T, \quad (\text{C2})$$

i.e., the expansion of the scattering maintains exactly the same formal expression independently of the choice of the eigenvector normalization constants.

-
- [1] J. Mehra and H. Reichenberg, *The historical development of quantum theory* (Springer, Berlin, 2001).
 - [2] C. Mahaux and H. A. Weidenmüller, *Shell-Model Approach to Nuclear Reactions* (North-Holland, Amsterdam, 1969).
 - [3] S. Datta, *Electronic Transport in Mesoscopic Systems* (Cambridge University Press, Cambridge, UK, 1995).
 - [4] H.-J. Stöckmann, *Quantum chaos: An introduction* (Cambridge University Press, Cambridge, UK, 1999).
 - [5] D. M. Pozar, *Microwave Engineering*, 4th ed. (Wiley, New York, 2012).
 - [6] C. Bohren and D. Huffman, *Absorption and Scattering of Light by Small Particles* (Wiley, New York, 1983).
 - [7] D. M. Whittaker and I. S. Culshaw, Phys. Rev. B **60**, 2610 (1999).
 - [8] M. Liscidini, D. Gerace, L. C. Andreani, and J. E. Sipe, Phys. Rev. B **77**, 035324 (2008).
 - [9] M. Nevière, R. Reinisch, and E. Popov, J. Opt. Soc. Am. A **12**, 513 (1995).
 - [10] S. G. Tikhodeev, A. L. Yablonskii, E. A. Muljarov, N. A. Gippius, and T. Ishihara, Phys. Rev. B **66**, 045102 (2002).
 - [11] P. T. Leung, S. Y. Liu, and K. Young, Phys. Rev. A **49**, 3057 (1994).
 - [12] E. A. Muljarov, W. Langbein, and R. Zimmermann, Europhys. Lett. **92**, 50010 (2010).
 - [13] P. T. Kristensen, C. V. Vlack, and S. Hughes, Opt. Lett. **37**, 1649 (2012).
 - [14] C. Sauvan, J. P. Hugonin, I. S. Maksymov, and P. Lalanne, Phys. Rev. Lett. **110**, 237401 (2013).
 - [15] E. A. Muljarov and W. Langbein, Phys. Rev. B **93**, 075417 (2016).
 - [16] S. Fan, W. Suh, and J. D. Joannopoulos, J. Opt. Soc. Am. A **20**, 569 (2003).
 - [17] C. W. Hsu, B. G. DeLacy, S. G. Johnson, J. D. Joannopoulos, and M. Soljačić, Nano Lett. **14**, 2783 (2014).
 - [18] R. Alaee, D. Lehr, R. Filter, F. Lederer, E.-B. Kley, C. Rockstuhl, and A. Tünnermann, ACS Photonics **2**, 1085 (2015).
 - [19] L. Verslegers, Z. Yu, Z. Ruan, P. B. Catrysse, and S. Fan, Phys. Rev. Lett. **108**, 083902 (2012).
 - [20] M. Decker, I. Staude, M. Falkner, J. Dominguez, D. N. Neshev, I. Brener, T. Pertsch, and Y. S. Kivshar, Adv. Opt. Mat. **3**, 813 (2015).
 - [21] S. Fan and J. D. Joannopoulos, Phys. Rev. B **65**, 235112 (2002).
 - [22] K. X. Wang, Z. Yu, S. Sandhu, and S. Fan, Opt. Lett. **38**, 100 (2013).
 - [23] D. A. Bykov and L. L. Doskolovich, Opt. Express **23**, 19234 (2015).
 - [24] W. Suh, Z. Wang, and S. Fan, IEEE J. Quantum Elect. **40**, 1511 (2004).
 - [25] E. Waks and J. Vuckovic, Opt. Express **13**, 5064 (2005).
 - [26] R. E. Hamam, A. Karalis, J. D. Joannopoulos, and M. Soljačić, Phys. Rev. A **75**, 053801 (2007).
 - [27] Z. Ruan and S. Fan, Phys. Rev. A **85**, 043828 (2012).
 - [28] R.-C. Ge, P. T. Kristensen, J. F. Young, and S. Hughes, New J. Phys. **16**, 113048 (2014).
 - [29] Q. Bai, M. Perrin, C. Sauvan, J.-P. Hugonin, and P. Lalanne, Opt. Express **21**, 27371 (2013).
 - [30] B. Vial, F. Zolla, A. Nicolet, and M. Commandré, Phys. Rev. A **89**, 023829 (2014).
 - [31] The discussion in this section can be generalized to more complex situations (for instance, different values of the background dielectric constant in the two half spaces), provided that the corresponding dyadic Green tensor is used in Eq. (4).
 - [32] D. C. Brody, J. Phys. A: Math. Theor. **47**, 035305 (2013).
 - [33] J. B. Conway, *Functions of One Complex Variable I* (Springer, New York, 1995).
 - [34] O. Bretscher, *Linear Algebra with Applications*, 4th ed. (Pearson, Upper Saddle River, NJ, 2009).
 - [35] V. Liu and S. Fan, Comput. Phys. Commun. **183**, 2233 (2012).
 - [36] COMSOL Multiphysics, <http://www.comsol.com>.
 - [37] See Supplemental Material at [URL] for a plot of the amplitude of selected quasinormal modes and a discussion of the convergence behavior of the computed transmittance with respect to the choice of the number of modes.
 - [38] J. Yang, J.-P. Hugonin, and P. Lalanne, ACS Photonics **3**, 395 (2016).
 - [39] W. Qiu, B. G. DeLacy, S. G. Johnson, J. D. Joannopoulos, and M. Soljačić, Opt. Express **20**, 18494 (2012).
 - [40] S. Lal, S. Link, and N. J. Halas, Nat. Photonics **1**, 641 (2007), and references therein.
 - [41] S. Jahani and Z. Jacob, Nat. Nanotech. **11**, 23 (2016).
 - [42] A. B. Klemm, D. Stellinga, E. R. Martins, L. Lewis, G. Huyet, L. O'Faolain, and T. F. Krauss, Opt. Lett. **38**, 3410 (2013).
 - [43] N. Yu and F. Capasso, Nat. Mater. **13**, 139 (2014).
 - [44] D. Lin, P. Fan, E. Hasman, and M. L. Brongersma, Science **345**, 298 (2014).
 - [45] P. Moitra, Y. Yang, Z. Anderson, I. I. Kravchenko, D. P. Briggs, and J. Valentine, Nat Photonics **7**, 791 (2013).
 - [46] V. A. Fedotov, P. L. Mladyonov, S. L. Prosvirnin, A. V. Rogacheva, Y. Chen, and N. I. Zheludev, Phys. Rev. Lett. **97**, 167401 (2006).
 - [47] C. Menzel, C. Helgert, C. Rockstuhl, E.-B. Kley, A. Tünnermann, T. Pertsch, and F. Lederer, Phys. Rev. Lett. **104**, 253902 (2010).
 - [48] A. Alù and N. Engheta, Phys. Rev. Lett. **100**, 113901 (2008).

Supplemental Material: Quasinormal-mode expansion of the scattering matrix

F. Alpeggiani,^{1,2} P. Nikhil,¹ E. Verhagen,¹ and L. Kuipers^{1,2}

¹*Center for Nanophotonics, FOM Institute AMOLF,
Science Park 104, 1098 XG Amsterdam, The Netherlands*

²*Kavli Institute of Nanoscience, Department of Quantum Nanoscience,
Delft University of Technology, Lorentzweg 1, 2628 CJ Delft, The Netherlands*
(Dated: November 18, 2016)

Here, we provide additional data on the convergence of the quasinormal-mode expansion of the scattering matrix with respect to the choice of the number of modes. We consider the same example as Sec. IIB in the main text.

In Fig. S1, we illustrate the effect of including an additional pair of leaky modes to the set employed in Sec. IIB and originally displayed in Fig. 3(a) of the main text. The additional modes, which are highlighted with an arrow in Fig. S1(a), have been computed from the complex-frequency poles of the transmission amplitude with the Fourier modal method [Ref. 35 in the main text]. As it can be seen from Fig. S1(b), the agreement between the total transmission predicted from our theory (red solid curve) and the simulated data (dashed curve) is further improved with respect to Fig. 3(b) in the main text, in agreement with the considerations on the completeness of the quasinormal-mode basis.

Incidentally, we notice that other choices of the set of electromagnetic modes could provide comparable accuracy in the prediction of the transmission properties. For instance, in Fig. S1(c,d) we show that, in this particular example, excluding the modes with $\text{Re}\tilde{\omega}_j < 0$ [see Fig. S1(c)] leads to an excellent agreement with the exact simulated data [Fig. S1(d)], without the need for including the additional pair of leaky modes discussed beforehand. The accuracy is probably due to the fact that the set of leaky modes in Fig. S1(c) is clearly symmetric with respect to the frequency

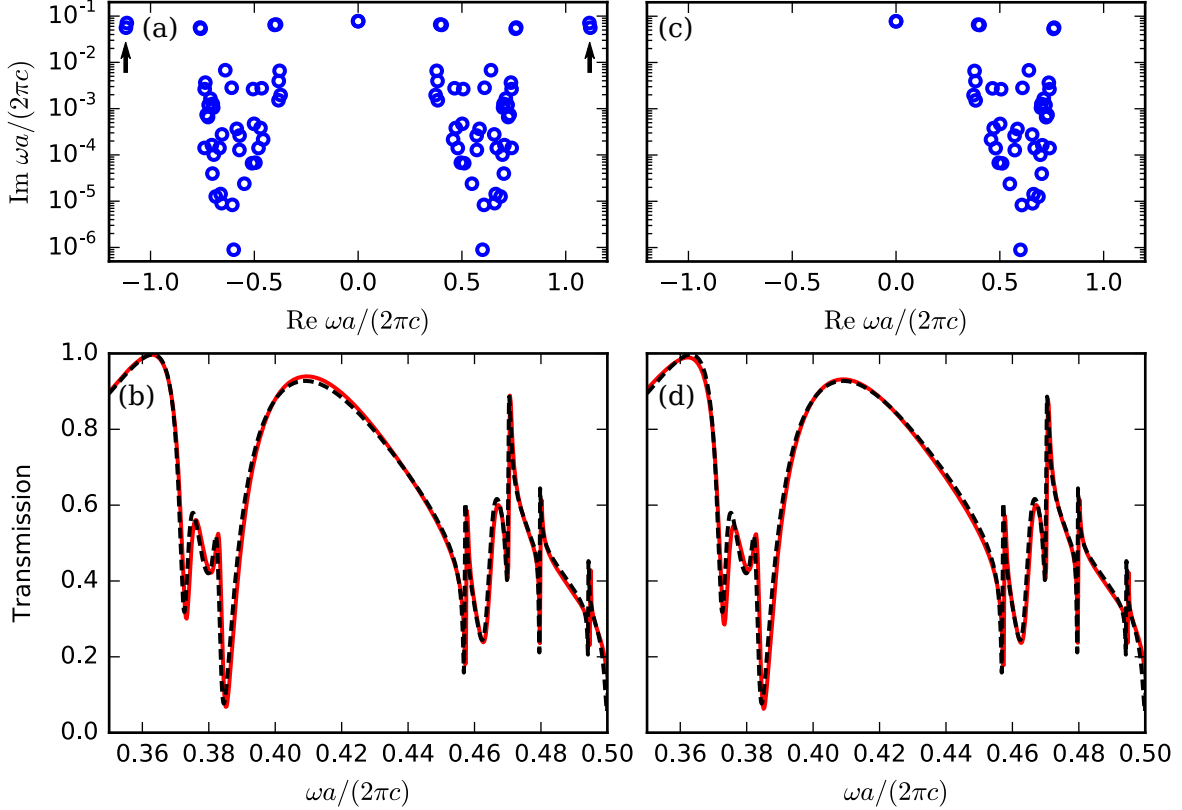


Figure S1. (a,c) Real and imaginary part (log scale) of different sets of the modal eigenfrequencies for the system considered in Sec. IIB in the main text. (b,d) Comparison of the total transmission computed by the quasinormal-mode expansion (solid red curve) with the exact result (dashed curve). Curves in (b) and (d) refer to the choices of the modes in (a) and (c), respectively.

range considered in Fig. S1(d), suggesting that, in some cases, the convergence behavior of the quasinormal-mode expansion could be enhanced by a suitable choice of the modes.

For illustration purposes, we also show in Fig. S2(a,b) a plot of the amplitude of the electric field of two quasinormal modes selected from those of Fig. 3(a) in the main text, computed with the finite-element method. The corresponding complex frequencies are indicated in the figure. The plot displays a region of the xz plane on the edge ($y = 0$) of the unit cell of the periodic photonic structure (see the schematic in Fig. 3(a) of the main text). The divergent behavior of the highly radiative quasinormal mode (b) is clearly recognizable.

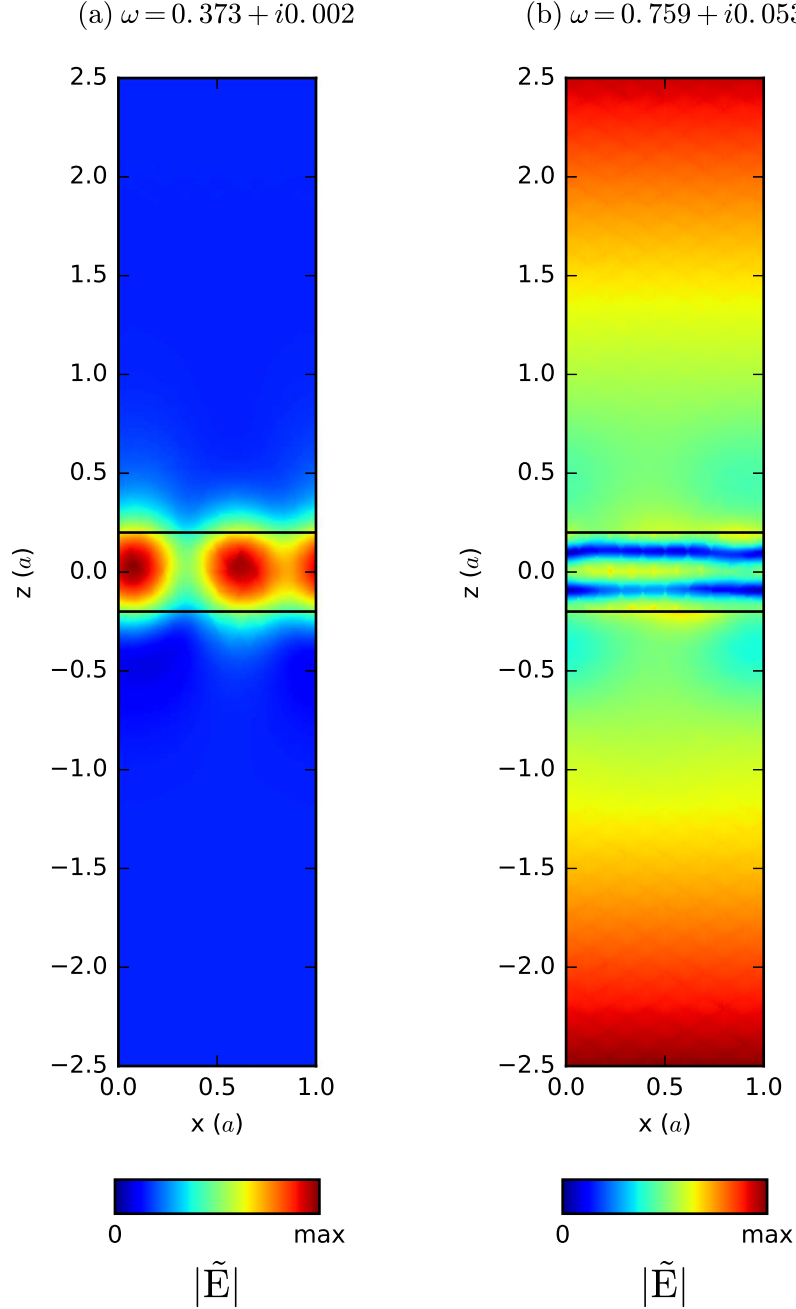


Figure S2. Amplitude of the electric field of two quasinormal modes selected from those of Fig. 3(a) in the main text. The plot shows a region of the xz plane along the edge of the unit cell close to the long side of the L-shaped structure ($y = 0$). The complex frequencies of the modes are: (a) $\omega a/(2\pi c) = 0.373 + i0.002$, and (b) $\omega a/(2\pi c) = 0.759 + i0.053$.